Molecular mechanisms of isocitrate dehydrogenase 1 (IDH1) mutations identified in tumors: the role of size and hydrophobicity at residue 132 on catalytic efficiency

Diego Avellaneda Matteo[1,‡], Adam J. Grunseth[1,‡], Eric R. Gonzalez[‡], Stacy L. Anselmo[‡], Madison A. Kennedy[‡], Precious Moman[‡], David A. Scott[§], An Hoang[‡], and Christal D. Sohl[‡,2]

From the [‡]Department of Chemistry and Biochemistry, San Diego State University, San Diego, CA 92182, and the [§]Sanford Burnham Prebys Medical Discovery Institute, La Jolla, CA 92037

[1]Both authors contributed equally to this work.
[2]To whom correspondence should be addressed: Prof. Christal D. Sohl, Department of Chemistry and Biochemistry, San Diego State University, CSL 328, MC1030, 5500 Campanile Dr., San Diego, California 92182, Telephone: (619) 594-2053; Fax: (619) 594-4634; Email: csohl@mail.sdsu.edu
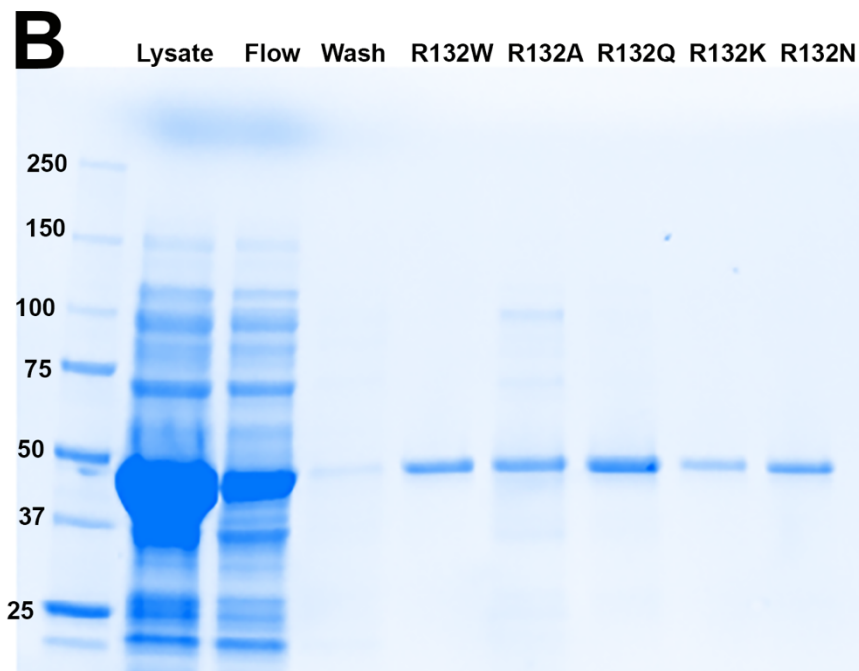
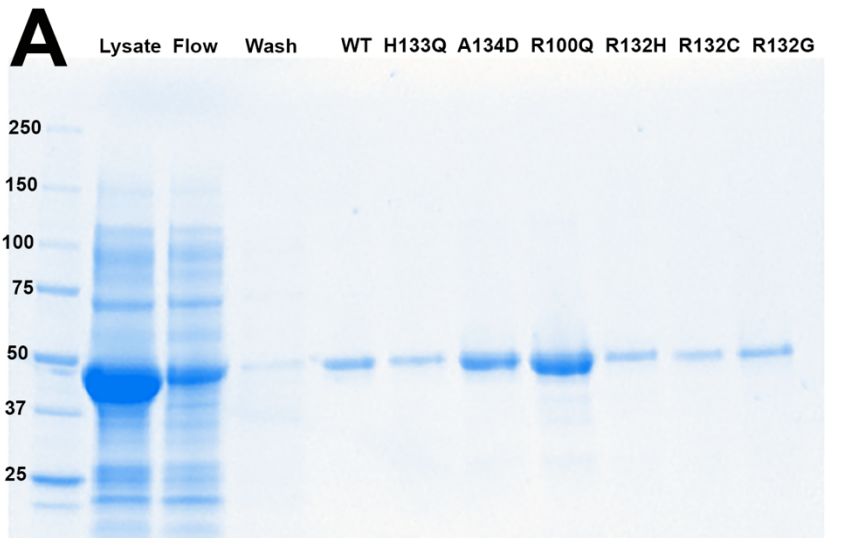**Supplemental methods content:**
Supplemental Figure S1
Supplemental Figure S2
Supplemental Figure S3
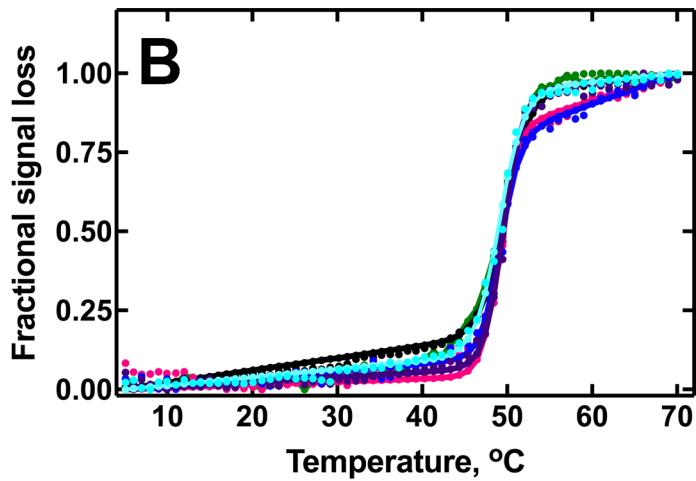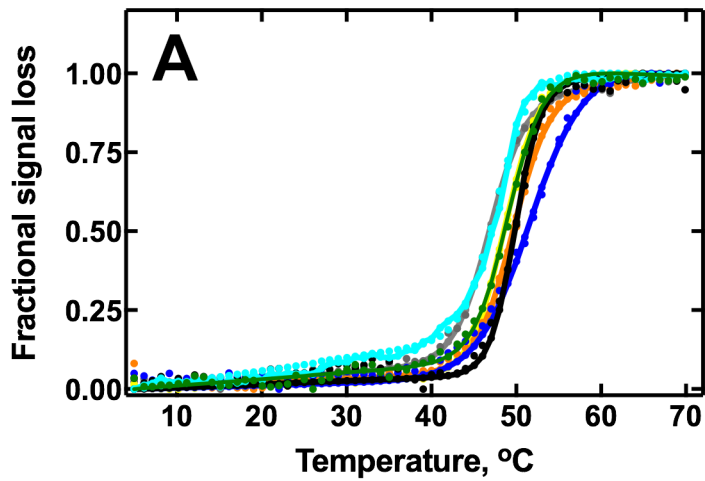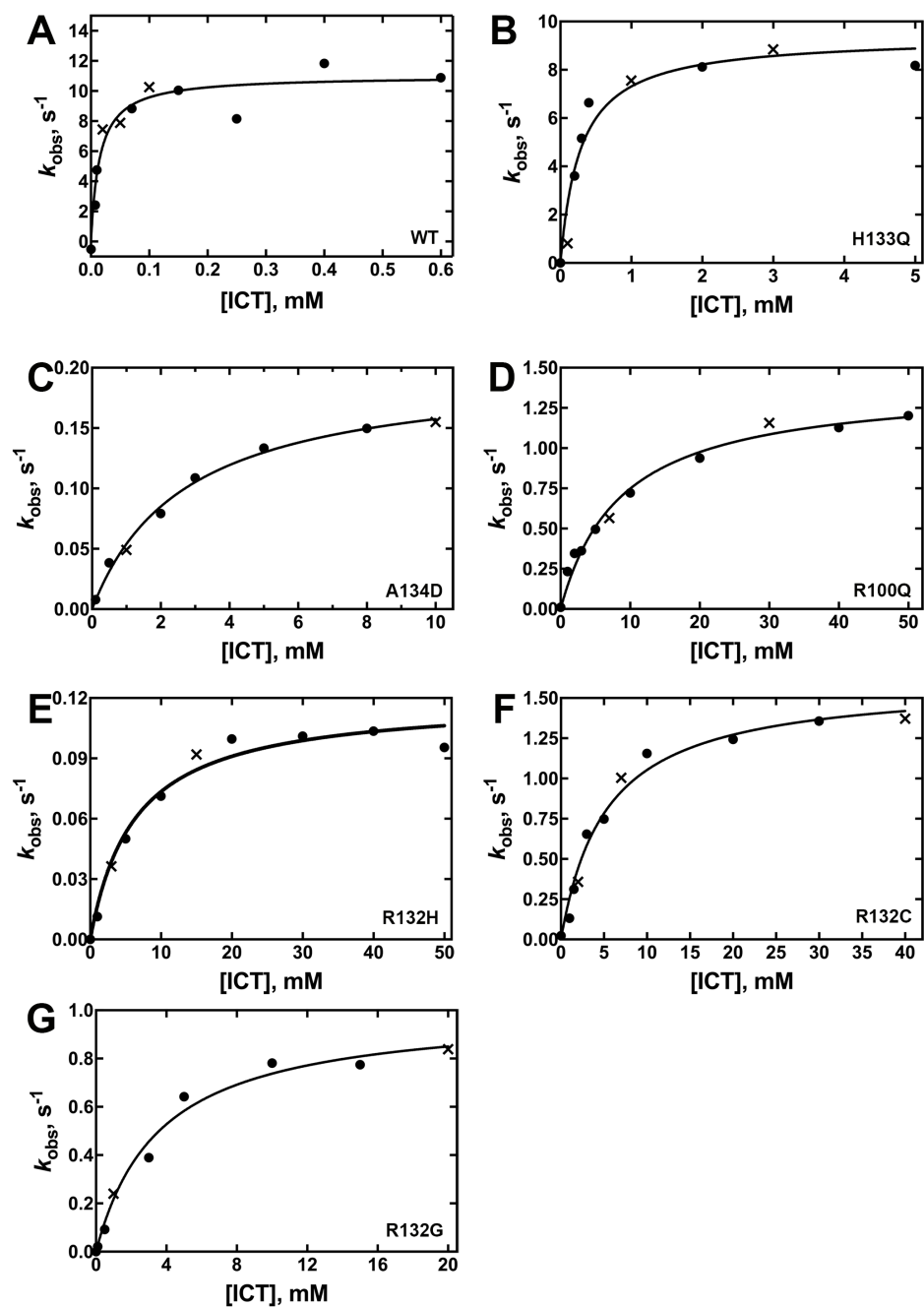Supplemental Figure S4
Supplemental Figure S5
Supplemental Figure S6

**Supplemental Figure S1.** Purification of WT and mutant IDH1. (A) SDS-PAGE analysis of the IDH1 tumor mutants. (B) SDS-PAGE analysis of the IDH1 experimental mutants. Lysate indicates the whole cell lysate, Flow indicates the flow-through after loading the lysate onto a nickel-NTA column, and Wash indicates the flow-through after a buffer wash prior to elution. 4-12% BioRad Stain-free gels were used.
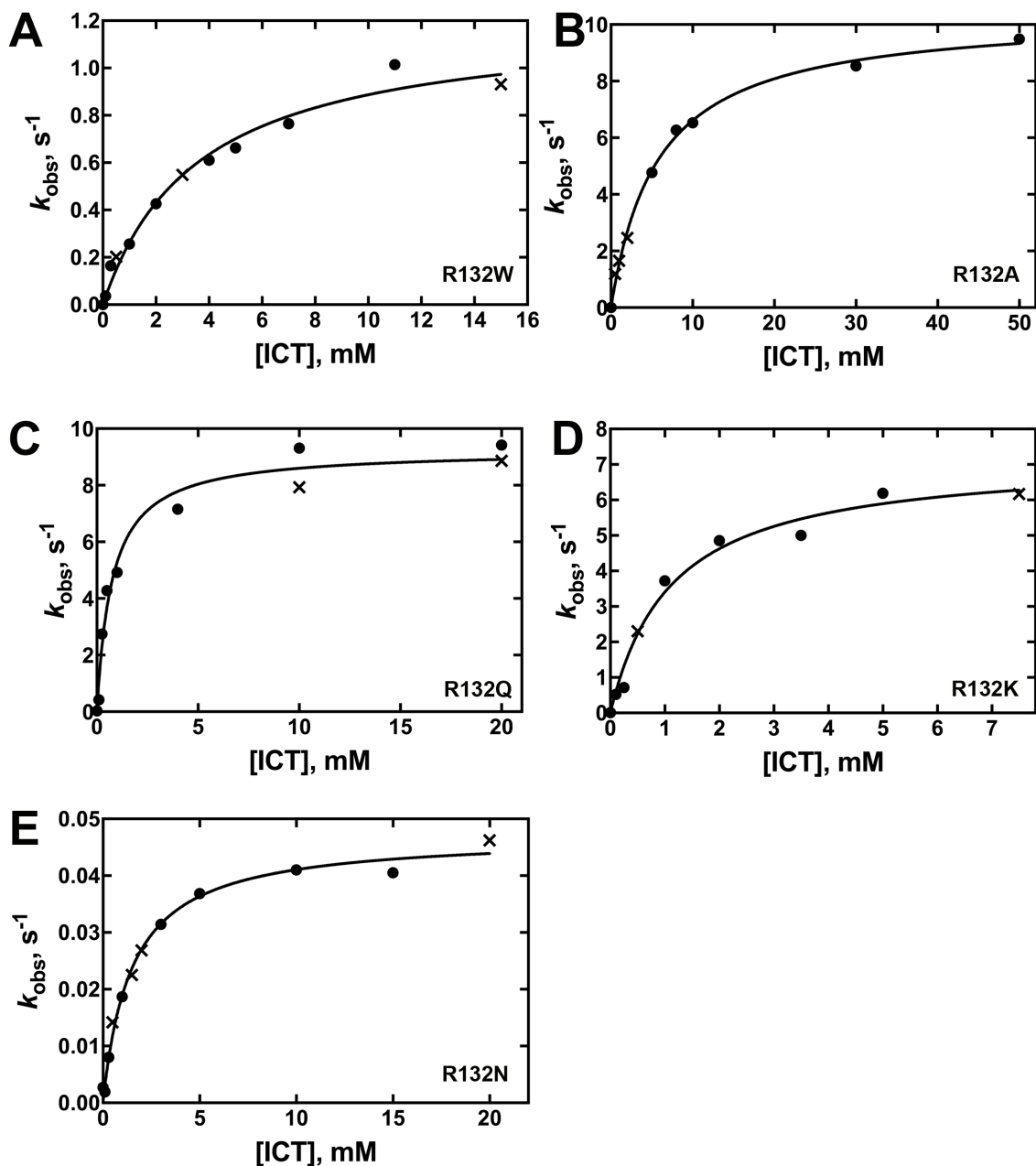
Supplemental Figure S2. Thermal melt curves employing circular dichroism were used to determine the melting temperature (T_m) of IDH1 mutants. (A) WT IDH1 is shown in green ($T_m = 49.1 \pm 0.1$ °C); A134D in cyan ($T_m = 48.7 \pm 0.1$ °C); H133Q in black ($T_m = 49.9 \pm 0.1$ °C); R100Q in dark blue ($T_m = 51.9 \pm 0.1$ °C); R132H in orange ($T_m = 49.7 \pm 0.1$ °C); R132C in yellow ($T_m = 46.8 \pm 0.1$ °C); and R132G in grey ($T_m = 46.9 \pm 0.1$ °C). (B) WT IDH1 is shown in green ($T_m = 49.1 \pm 0.1$ °C); R132W is in purple ($T_m = 49.5 \pm 0.1$ °C); R132A in dark blue ($T_m = 49.2 \pm 0.1$ °C); R132N in cyan ($T_m = 49.1 \pm 0.1$ °C); R132Q in magenta ($T_m = 49.0 \pm 0.1$ °C); and R132K in black ($T_m = 49.8 \pm 0.1$ °C).
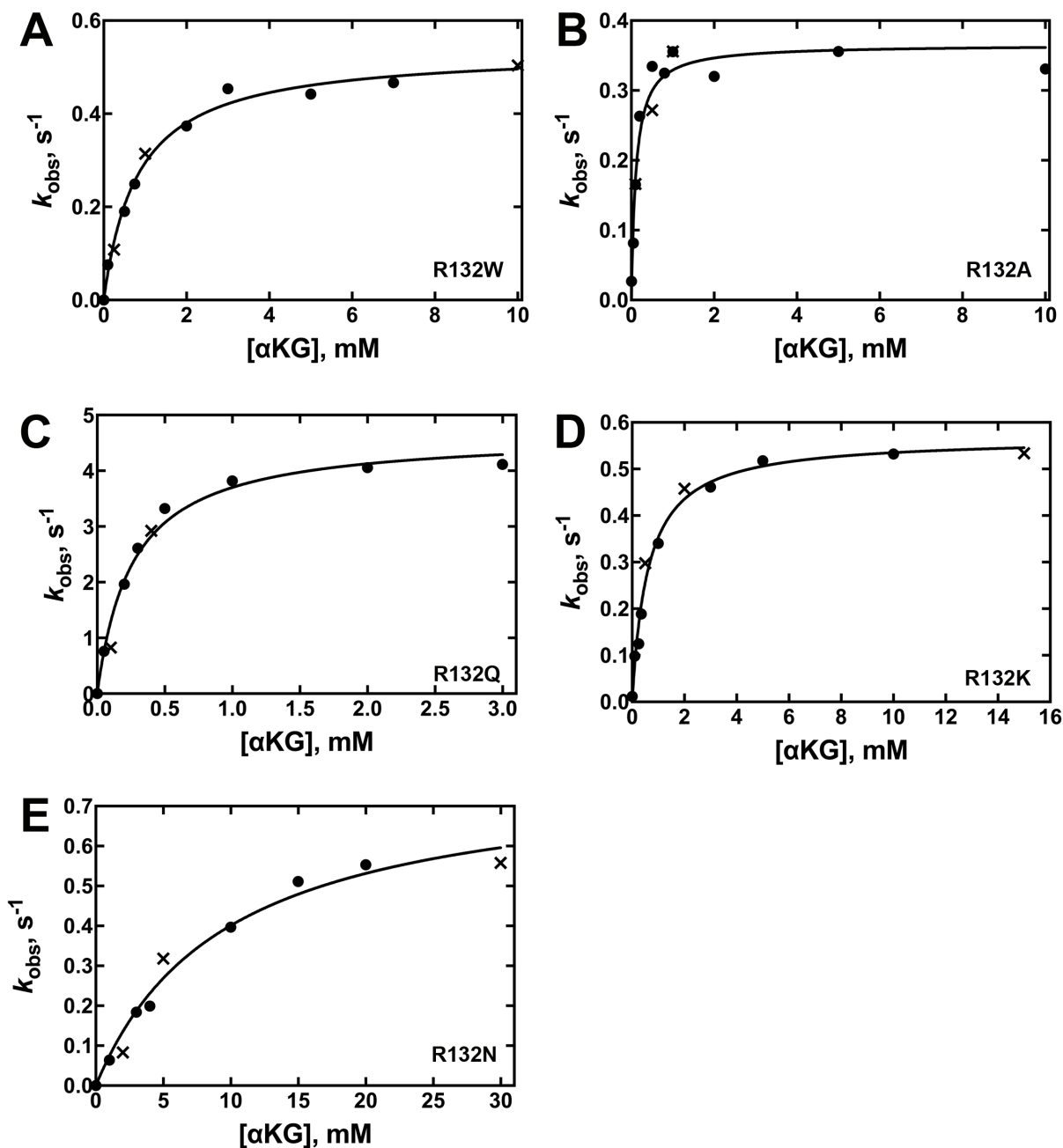
Supplemental Figure S3. Concentration dependence of ICT concentration on the observed rate of NADPH production in the normal reaction, conversion of ICT to αKG (21 °C). The determined k_{obs} values were obtained from two different enzyme preparations to ensure reproducibility. The k_{obs} values resulting from each of the two enzyme preparations are distinguished by using either a circle or an × in the plots. The observed rate constants (k_{obs}) were calculated from the linear range of the slopes of plots of concentration versus time using GraphPad Prism software (GraphPad, San Diego, CA.) These k_{obs} values were then fit to a hyperbolic equation to generate k_{cat} and K_m values, and the standard error results from the deviance from these hyperbolic fits is indicated. K_m values and efficiency are in terms of [ICT]. (A) WT IDH1. (B) H133Q IDH1. (C) A134D IDH1. (D) R100Q IDH1. (E) R132H IDH1. (F) R132C IDH1. (G) R132G IDH1.
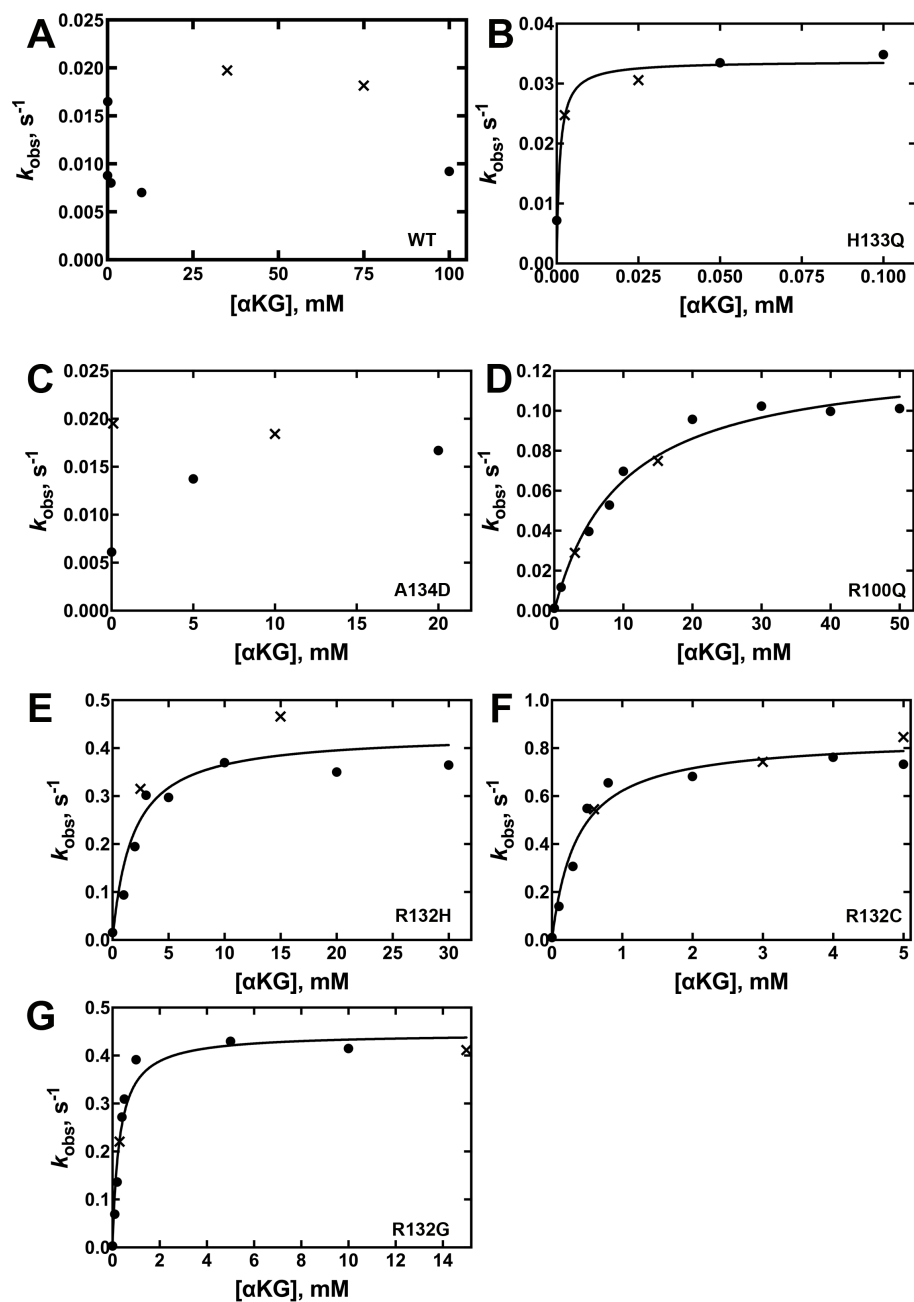
Supplemental Figure S4. Concentration dependence of αKG concentration on the observed rate of NADPH depletion in the neomorphic reaction, conversion of αKG to D2HG (21 °C). The determined k_{obs} values were obtained from two different enzyme preparations to ensure reproducibility. The k_{obs} values resulting from each of the two enzyme preparations are distinguished by using either a circle or an × in the plots. The observed rate constants (k_{obs}) were calculated from the linear range of the slopes of plots of concentration versus time using GraphPad Prism software (GraphPad, San Diego, CA). These k_{obs} values were then fit to a hyperbolic equation to generate k_{cat} and K_m values, and the standard error results from the deviance from these hyperbolic fits is indicated. K_m values and efficiency are in terms of [αKG]. (A) WT IDH1. (B) H133Q IDH1. (C) A134D IDH1. (D) R100Q IDH1. (E) R132H IDH1. (F) R132C IDH1. (G) R132G IDH1.

Supplemental Figure S5. Concentration dependence of ICT concentration on the observed rate of NADPH production in the normal reaction, conversion of ICT to αKG (37 ºC). The determined k_{obs} values were obtained from two different enzyme preparations to ensure reproducibility. The k_{obs} values resulting from each of the two enzyme preparations are distinguished by using either a circle or an × in the plots. The observed rate constants (k_{obs}) were calculated from the linear range of the slopes of plots of concentration versus time using GraphPad Prism software (GraphPad, San Diego, CA). These k_{obs} values were then fit to a hyperbolic equation to generate k_{cat} and K_m values, and the standard error results from the deviance from these hyperbolic fits is indicated. K_m values and efficiency are in terms of [ICT]. (A) R132W IDH1. (B) R132A IDH1. (C) R132Q IDH1. (D) R132K IDH1. (E) R132N IDH1.

Supplemental Figure S6. Concentration dependence of αKG concentration on the observed rate of NADPH depletion in the neomorphic reaction, conversion of αKG to D2HG (37 °C). The determined k_{obs} values were obtained from two different enzyme preparations to ensure reproducibility. The k_{obs} values resulting from each of the two enzyme preparations are distinguished by using either a circle or an × in the plots. The observed rate constants (k_{obs}) were calculated from the linear range of the slopes of plots of concentration versus time using GraphPad Prism software (GraphPad, San Diego, CA). These k_{obs} values were then fit to a hyperbolic equation to generate k_{cat} and K_m values, and the standard error results from the deviance from these hyperbolic fits is indicated. K_m values and efficiency are in terms of [αKG]. (A) R132W IDH1. (B) R132A IDH1. (C) R132Q IDH1. (D) R132K IDH1. (E) R132N IDH1.